

# Enhanced Immunotherapeutic Efficacy of Anti-PD-L1 Antibody in Combination with an EP4 Antagonist

Yamato Sajiki,\* Satoru Konnai,\*<sup>†</sup> Zimeng Cai,<sup>‡</sup> Kensuke Takada,<sup>‡</sup> Tomohiro Okagawa,<sup>†</sup> Naoya Maekawa,<sup>†</sup> Sotaro Fujisawa,\* Yukinari Kato,<sup>§,¶</sup> Yasuhiko Suzuki,<sup>‡,||</sup> Shiro Murata,\*<sup>†</sup> and Kazuhiko Ohashi\*<sup>†</sup>

\*Department of Disease Control, Faculty of Veterinary Medicine, Hokkaido University, Sapporo 060-0818, Japan; <sup>†</sup>Department of Advanced Pharmaceutics, Faculty of Veterinary Medicine, Hokkaido University, Sapporo 060-0818, Japan; <sup>‡</sup>Department of Applied Veterinary Sciences, Faculty of Veterinary Medicine, Hokkaido University, Sapporo 060-0818, Japan; <sup>§</sup>Department of Antibody Drug Development, Tohoku University Graduate School of Medicine, Sendai 980-8575, Japan; <sup>¶</sup>New Industry Creation Hatchery Center, Tohoku University, Sendai 980-8575, Japan; and <sup>||</sup>Division of Bioresources, Research Center for Zoonosis Control, Hokkaido University, Sapporo 001-0019, Japan

## ABSTRACT

Combination treatment approaches are increasingly considered to overcome resistance to immunotherapy targeting immunoinhibitory molecules such as programmed death (PD)-1 and PD-ligand 1 (PD-L1). Previous studies have demonstrated that the therapeutic efficacy of anti-PD-L1 Abs is enhanced by combination treatment with cyclooxygenase-2 inhibitors, through downregulation of the immunosuppressive eicosanoid PGE<sub>2</sub>, although the underlying mechanism remains unclear. In this study, we show that serum PGE<sub>2</sub> levels are upregulated after anti-PD-L1 Ab administration in a bovine model of immunotherapy and that PGE<sub>2</sub> directly inhibits T cell activation via its receptor E prostanoic acid (EP) 4. Additionally, anti-PD-L1 Ab induces TNF- $\alpha$  production and TNF- $\alpha$  blockade reduces PGE<sub>2</sub> production in the presence of anti-PD-L1 Ab, suggesting that anti-PD-L1 Ab-induced TNF- $\alpha$  impairs T cell activation by PGE<sub>2</sub> upregulation. Our studies examining the therapeutic potential of the dual blockade of PD-L1 and EP4 in bovine and murine immune cells reveal that the dual blockade of PD-L1 and EP4 significantly enhances Th1 cytokine production in vitro. Finally, we show that the dual blockade decreases tumor volume and prolongs survival in mice inoculated with the murine lymphoma cell line EG7. Altogether, these results suggest that TNF- $\alpha$  induced by anti-PD-L1 Ab treatment is associated with T cell dysfunction via PGE<sub>2</sub>/EP4 pathway and that the dual blockade of PD-L1 and EP4 should be considered as a novel immunotherapy for cancer. *ImmunoHorizons*, 2020, 4: 837–850.

Received for publication October 18, 2020. Accepted for publication November 10, 2020.

**Address correspondence and reprint requests to:** Dr. Satoru Konnai, Department of Disease Control, Faculty of Veterinary Medicine, Hokkaido University, Kita-18 Nishi-9, Kita-ku, Sapporo 060-0818, Japan. E-mail address: konnai@vetmed.hokudai.ac.jp

ORCID: 0000-0003-1237-4686 (Z.C.); 0000-0002-1391-9732 (T.O.); 0000-0001-5385-8201 (Y.K.); 0000-0002-1313-1494 (Y. Suzuki).

The microarray data presented in this article have been submitted to ArrayExpress (<https://www.ebi.ac.uk/arrayexpress/>) under accession number E-MTAB-9576.

This work was supported by Grants-in-Aid for Scientific Research and a Japan Society for the Promotion of Science (JSPS) Research Fellowship, Research Project for Improving Animal Disease Prevention Technologies to Combat Antimicrobial Resistance 2017–2021 FY of the Ministry of Agriculture, and grants from the Project of the NARO, Bio-oriented Technology Research Advancement Institution (Research Program on Development of Innovative Technology 26058 BC [to S.K.] and Special Scheme Project on Regional Developing Strategy Grant 16817557 [to S.K.]). The funders had no role in study design, data collection and analysis, decision to publish, or preparation of the manuscript.

Y. Sajiki performed most of the experiments, analyzed the data, prepared figures, and wrote the manuscript. S.K. conceived and designed experiments, analyzed the data, and revised the manuscript. Z.C. and K.T. assisted in the experimental design and the experiments using the murine tumor model and revised the manuscript. T.O. and N.M. helped with immunological analyses using bovine immune cells, analyzed the data, and assisted in manuscript writing. S.F., Y.K., and Y. Suzuki provided laboratory materials and reagents. S.M. and K.O. assisted in the experimental design and revised the manuscript. All authors reviewed and approved the final manuscript.

**Abbreviations used in this article:** BLV, bovine leukemia virus; COX, cyclooxygenase; EP, E prostanoic acid; FLK, fetal lamb kidney; PD, programmed death; PD-L1, PD-ligand 1; qPCR, quantitative real-time PCR; TNFR11, TNF receptor type II.

The online version of this article contains supplemental material.

This article is distributed under the terms of the [CC BY-NC-ND 4.0 Unported license](https://creativecommons.org/licenses/by-nc-nd/4.0/).

Copyright © 2020 The Authors

<https://doi.org/10.4049/immunohorizons.2000089>

*ImmunoHorizons* is published by The American Association of Immunologists, Inc.

## INTRODUCTION

Programmed death (PD)-1 is an immune checkpoint molecule that negatively regulates T cell function via the interaction with its ligands, PD-ligand 1 (PD-L1) and PD-L2 (1). Upregulation of PD-1 plays a key role in T cell exhaustion, and PD-1/PD-L1 pathway is involved in the progression of a variety of tumors and chronic infections (2, 3). In contrast, previous reports have demonstrated that the inhibition of the PD-1/PD-L1 pathway using specific Abs restores the effector functions of exhausted T cells and enhances antitumor immune responses (4–6). Therefore, the immunotherapy targeting the PD-1/PD-L1 pathway has become a promising therapeutic strategy for the treatment of patients with tumors (7, 8). Recently, studies have also demonstrated the efficacy of PD-1/PD-L1 blockade in the field of veterinary medicine (9–13). We have previously shown the therapeutic potential of anti-PD-1/PD-L1 Abs for the treatment of bovine leukemia virus (BLV)-infected cattle (9, 10, 12). BLV, an oncogenic deltaretrovirus of cattle that is closely related to human T cell leukemia virus type 1, infects B cells, and 1–5% of BLV-infected cattle develop fatal lymphoma or lymphosarcoma after a long latent period (14, 15). After the administration of anti-PD-1/PD-L1 Abs, BLV proviral loads were significantly reduced in peripheral blood (9, 10, 12), suggesting that this strategy might contribute to a reduced risk of tumorigenesis associated with BLV infection.

Although the immunotherapy targeting the PD-1/PD-L1 pathway have been approved for cancer treatment in humans, a significant proportion of the patients remains less responsive (16). A potential strategy to overcome this issue is combining anti-PD-1/PD-L1 Abs with other therapies. PGE<sub>2</sub> is one of the candidate targets for combination treatment with anti-PD-1/PD-L1 Abs. PGE<sub>2</sub> is known as an inflammatory mediator derived from arachidonic acid by cyclooxygenase (COX)-1, COX-2, and PGE synthases (17). COX-1 is a constitutive enzyme and widely expressed in many tissues, whereas COX-2 is an inducible enzyme whose expression is regulated by the activation of NF- $\kappa$ B by inflammatory cytokines and growth factors (18, 19). There are four PGE<sub>2</sub> receptors, E prostanoïd (EP) 1, EP2, EP3, and EP4 (20). PGE<sub>2</sub> inhibits the activity of immune cells, such as T cells, dendritic cells, and NK cells, via EP2 and EP4 receptors (21). In addition, numerous studies have demonstrated the role of COX2/PGE<sub>2</sub> in tumor microenvironments (22). The increased expression of COX-2 in breast and colorectal cancers is associated with poor prognosis (23, 24). In the tumor microenvironment, many cell types, including tumor cells and endothelial cells, produce PGE<sub>2</sub> via COX-2 activation, and PGE<sub>2</sub> enhances tumor cell progression via several pathways such as angiogenesis (25–27). In addition, PGE<sub>2</sub> affects the immune cells in tumor microenvironments. Specifically, PGE<sub>2</sub> regulates the activity of Th1 cells, whereas it enhances the function of immunosuppressive cells, such as regulatory T cells (21, 28). Interestingly, several studies have reported the role of PGE<sub>2</sub> as an inducer of PD-L1 expression. PGE<sub>2</sub> upregulates the expression of PD-L1 in murine and bovine models (29–31), and treatment with a COX-2 inhibitor reduces PD-L1

expression in an in vitro murine model (29). Furthermore, combination treatment with aspirin, a COX inhibitor, and anti-PD-1 Ab has been shown to suppress tumor growth in several murine tumor models (32). We have previously shown that combination treatment with anti-PD-L1 Ab and a COX-2 inhibitor has a significantly enhanced therapeutic efficacy in BLV-infected cattle (12), although the underlying mechanisms have not been fully elucidated.

In the current study, we focused on the function of PGE<sub>2</sub>, which is upregulated after the administration of anti-PD-L1 Abs in BLV-infected cattle. Our analyses using bovine immune cells revealed that PGE<sub>2</sub> directly suppressed the activity of T cells via EP4. In addition, TNF- $\alpha$  induced by anti-PD-L1 Ab treatment upregulated PGE<sub>2</sub> production from PBMCs. These findings revealed that the PGE<sub>2</sub>/EP4 axis might be a mechanism underlying resistance to anti-PD-L1 Ab treatment. Furthermore, our investigation in a murine lymphoma model revealed the therapeutic potential of combination treatment with anti-PD-L1 Ab and an EP4 antagonist based on the inhibition of tumor growth and prolonged survival in tumor-bearing mice, suggesting that the combination treatment should be considered as a novel immunotherapeutic approach in cancer.

## MATERIALS AND METHODS

### Cells

Blood samples derived from BLV-infected and -uninfected cattle were collected at several farms in Hokkaido, Japan, and BLV infection was diagnosed as described previously (33). Informed consent was obtained from all owners of cattle sampled in the current study. PBMCs were separated from the blood samples by density gradient centrifugation on Percoll (GE Healthcare, Little Chalfont, U.K.). For isolation of CD3<sup>+</sup> and CD4<sup>+</sup> cells, PBMCs from BLV-uninfected cattle were incubated with anti-bovine CD3 mAb (MM1A; Washington State University mAb Center, Pullman, WA) or anti-bovine CD4 mAb (CC8; Bio-Rad Laboratories, Hercules, CA) at 4°C for 30 min, followed by incubation with anti-mouse IgG<sub>1</sub> MicroBeads (Miltenyi Biotec, Bergisch Gladbach, Germany) at 4°C for 15 min. CD3<sup>+</sup> and CD4<sup>+</sup> cells were sorted from the PBMCs using AutoMACS Pro (Miltenyi Biotec), according to the manufacturer's protocol. The purity of cells, confirmed using FACS Verse (BD Biosciences, San Jose, CA), was routinely >90%. PBMCs and isolated CD3<sup>+</sup> and CD4<sup>+</sup> cells were cultured in 200  $\mu$ l RPMI 1640 medium (Sigma-Aldrich, St. Louis, MO) supplemented with 10% heat-inactivated FCS (Thermo Fisher Scientific, Waltham, MA), 100 U/ml penicillin (Thermo Fisher Scientific), 100  $\mu$ g/ml streptomycin (Thermo Fisher Scientific), and 2 mM L-glutamine (Thermo Fisher Scientific). All bovine cell cultures were grown in 96-well plates (Corning, Corning, NY) at 37°C under 5% CO<sub>2</sub> atmosphere.

Eight-week-old female BALB/c mice were purchased from Sankyo Labo Service Corporation (Tokyo, Japan) and sacrificed by isoflurane inhalation and cervical dislocation. The spleens were collected, minced with scissors, digested in RPMI 1640 medium

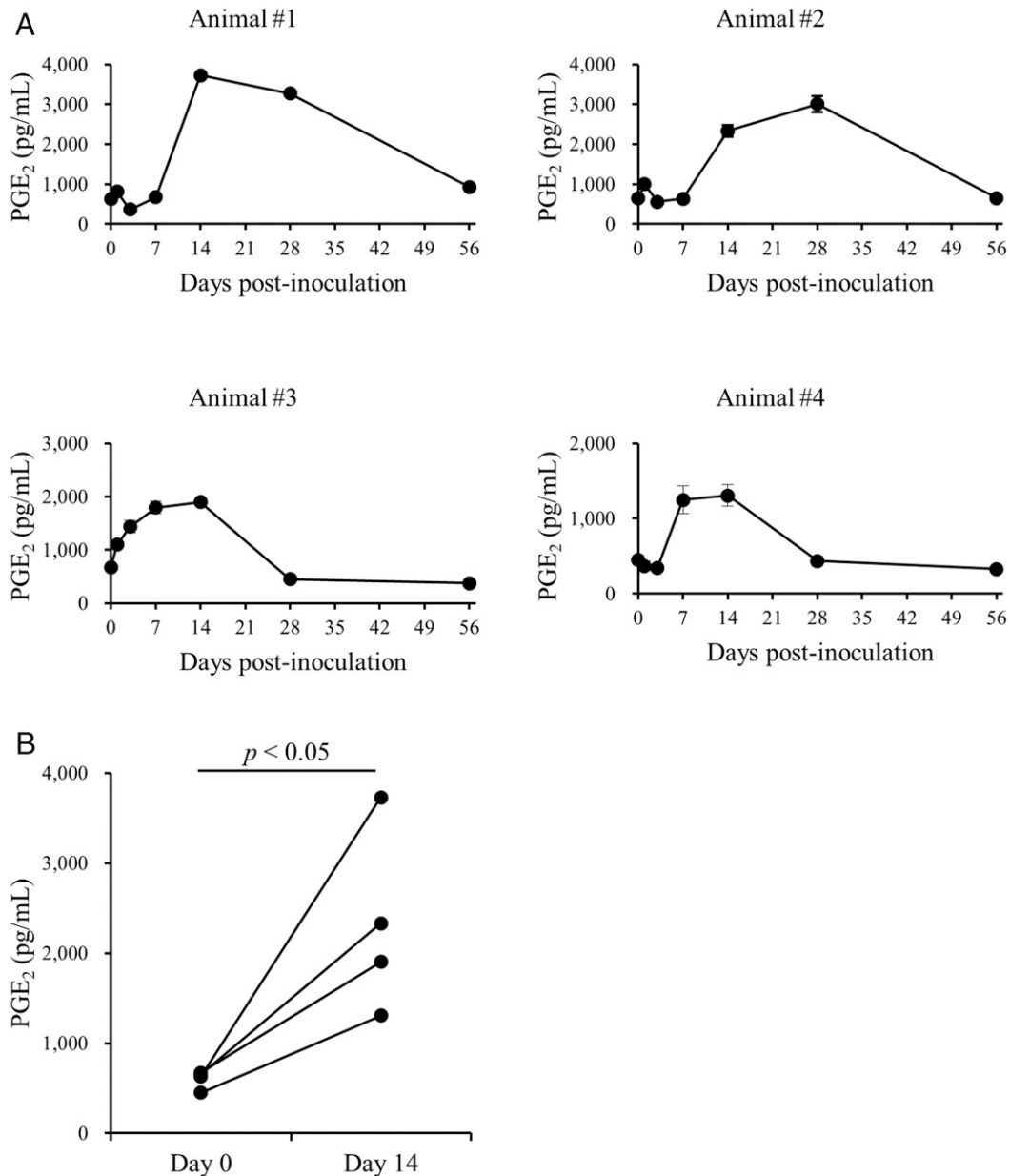


**FIGURE 1. Changes in serum PGE<sub>2</sub> concentrations after anti-PD-L1 Ab inoculation.**

(A and B) BLV-infected cattle (animals 1–4) were administered 1 mg/kg anti-PD-L1 Ab (Boch4G12), and serum samples were collected on days 0, 1, 3, 7, 14, 28, and 56. Serum PGE<sub>2</sub> concentrations were measured by ELISA. (B) Statistical significance was determined by the Mann-Whitney *U* test.

containing 0.2 mg/ml DNase I (Sigma-Aldrich) and 0.67 U/ml research-grade Liberase DL (Sigma-Aldrich) for 30 min at 37°C, and passed through a 100- $\mu$ m cell strainer (BD Biosciences). Next, the cells were washed twice with PBS and passed through a 40- $\mu$ m cell strainer (BD Biosciences). The isolated splenocytes were then cultured in culture medium as described above.

EG7 murine T cell lymphoma cell line (34) was obtained from American Type Culture Collection (Manassas, VA) and maintained in RPMI 1640 medium supplemented with 10% heat-inactivated FBS (Sigma-Aldrich), 1% penicillin-streptomycin

(FUJIFILM Wako Pure Chemical Corporation, Osaka, Japan), and 0.4 mg/ml G418 (FUJIFILM Wako Pure Chemical Corporation) at 37°C under 5% CO<sub>2</sub> atmosphere.

#### Serum samples

Four BLV-infected cattle (animals 1–4) were i.v. administered 1 mg/kg anti-bovine PD-L1 Ab (Boch4G12, a rat-bovine chimeric Ab) (9). Serum samples of the cattle obtained on days 0, 1, 3, 7, 14, 28, and 56 were stored at –80°C until use in the experiments. All experimental procedures using cattle were conducted following

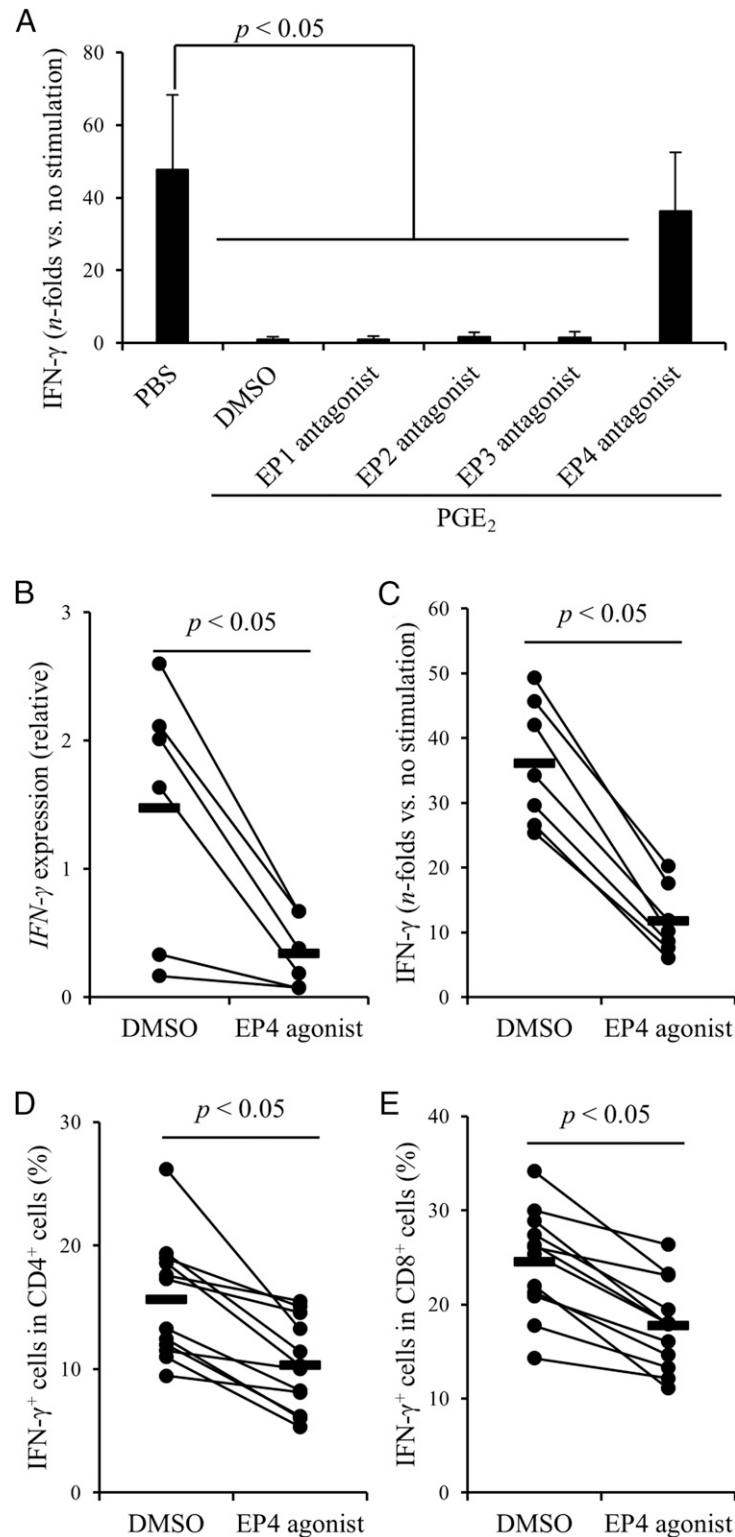


**FIGURE 2. Functional analysis of EP signaling in PBMCs.**

(A) Following an hour of incubation with indicated EP antagonists, PBMCs from BLV-uninfected cattle ( $n = 6$ ) were incubated with PGE<sub>2</sub> in the presence of anti-CD3 mAb and anti-CD28 mAb. After incubation, IFN- $\gamma$  concentrations in culture supernatants were determined by ELISA. (B) PBMCs from BLV-uninfected cattle ( $n = 6$ ) were cultured with the EP4 agonist, and the expression of mRNA-encoding IFN- $\gamma$  was quantitated by qPCR. DMSO was used as a vehicle control. (C) PBMCs from BLV-uninfected cattle ( $n = 7$ ) were incubated with the EP4 agonist in the presence of anti-CD3 mAb and anti-CD28 mAb. After incubation, IFN- $\gamma$  concentrations in culture supernatants were determined by ELISA. **(Continued)**

TABLE I. Cattle used in this study

|                     | Animal 1      | Animal 2      | Animal 3      | Animal 4      |
|---------------------|---------------|---------------|---------------|---------------|
| Age                 | 13 mo old     | 17 mo old     | 76 mo old     | 7 mo old      |
| Breed               | Holstein      | Holstein      | Holstein      | Holstein      |
| Sex                 | female        | female        | female        | male          |
| Body weight         | 295 kg        | 522 kg        | 799 kg        | 267 kg        |
| BLV infection       | +             | +             | +             | +             |
| Administration dose | 1 mg/kg, i.v. | 1 mg/kg, i.v. | 1 mg/kg, i.v. | 1 mg/kg, i.v. |

approval from the local committee for animal studies at Hokkaido University (approval number 17-0024).

### Quantitative real-time PCR

Quantitative real-time PCR (qPCR) was performed as described previously (30). Briefly, total RNA was extracted from cultured cells using TRI Reagent (Molecular Research Center, Cincinnati, OH) and cDNA was synthesized from the total RNA by Prime-Script Reverse Transcriptase (TaKaRa Bio, Otsu, Japan) following the manufacturers' protocols. Next, qPCR was performed using a LightCycler 480 System II (Roche Diagnostics, Mannheim, Germany) with SYBR Premix DimerEraser (TaKaRa Bio), following the manufacturers' protocols.  $\beta$ -actin (*ACTB*) was used as a reference gene, and relative expression levels were calculated using the  $\Delta\Delta$  cycle threshold method. The primers were 5'-ATA ACC AGG TCA TTC AAA GG-3' and 5'-ATT CTG ACT TCT CTT CCG CT-3' for bovine *IFN- $\gamma$* , 5'-ACG TTT TCT CGT GAA GCC CT-3' and 5'-TCT ACC AGA AGG GCG GGA TA-3' for bovine *COX2*, and 5'-TCT TCC AGC CTT CCT TCC TG-3' and 5'-ACC GTG TTG GCG TAG AGG TC-3' for bovine *ACTB*.

### ELISA

PGE<sub>2</sub> concentrations in sera and culture supernatants were measured by PG E<sub>2</sub> Express ELISA Kit (Cayman Chemical, Ann Arbor, MI), following the manufacturer's instructions. Bovine IFN- $\gamma$  and mouse IL-2 concentrations in culture supernatants were measured by Bovine IFN- $\gamma$  ELISA Development Kit (Mabtech, Nacka Strand, Sweden) and Mouse IL-2 Matched Ab Pair Kit (Abcam, Cambridge, U.K.), respectively, according to the manufacturers' protocols.

### Flow cytometry

For CD69 expression levels, collected cells were incubated in PBS containing 10% goat serum (Thermo Fisher Scientific) for 15 min at 25°C to prevent nonspecific reactions. Next, the cells were stained for 20 min at 25°C using the following Abs: FITC-conjugated anti-bovine CD4 mAb (CC8), PE-conjugated anti-bovine CD8 mAb (CC63; Bio-Rad Laboratories), and Alexa Fluor 647-labeled anti-bovine CD69 mAb (KTSN7A; Kingfisher Biotech, St. Paul, MN). KTSN7A was prelabeled with a Zenon Alexa Fluor 647 Mouse IgG<sub>1</sub>

Labeling Kit (Thermo Fisher Scientific). The stained cells were washed twice and analyzed immediately by FACS Verse.

For the intracellular staining of IFN- $\gamma$  and TNF- $\alpha$ , the collected cells were incubated in PBS containing 10% goat serum as described above, followed by staining with FITC-conjugated anti-bovine CD4 mAb (CC8), PerCP/Cy5.5-conjugated anti-bovine CD8 mAb (CC63), and PE-labeled anti-bovine IgM mAb (IL-A30; Bio-Rad Laboratories) for 20 min at 25°C. IL-A30 was prelabeled with a Zenon R-PE Mouse IgG<sub>1</sub> Labeling Kit (Thermo Fisher Scientific). CC63 was conjugated with PerCP/Cy5.5 by using a Lightning-Link Ab Labeling Kit (Innova Biosciences, Cambridge, U.K.). After surface staining, the cells were fixed and permeabilized using FOXP3 Fix/Perm Kit (BioLegend, San Diego, CA). Next, the cells were stained with biotinylated anti-bovine IFN- $\gamma$  mAb (MT307; Mabtech) or biotinylated anti-bovine TNF- $\alpha$  mAb (CC328; Bio-Rad Laboratories) for 20 min at 25°C. The cells were then incubated with allophycocyanin-conjugated streptavidin (BioLegend) for 20 min at 25°C. After the final staining, the cells were washed twice and analyzed immediately by FACS Verse.

### PBMC culture

To examine the individual effects of EP antagonists, PBMCs from BLV-uninfected cattle were incubated for 1 h with 1  $\mu$ g/ml of each of the following EP antagonists from Cayman Chemical: EP1 (SC-19220), EP2 (AH6809), EP3 (L-798,106), and EP4 (ONO-AE3-208), and then 250 nM PGE<sub>2</sub> (Cayman Chemical) was added to each culture. The PBMCs were stimulated by adding 1  $\mu$ g/ml anti-bovine CD3 mAb (MM1A) and 1  $\mu$ g/ml anti-bovine CD28 mAb (CC220; Bio-Rad Laboratories) to each well. After 24 h, the culture supernatants were collected to measure IFN- $\gamma$  concentrations by ELISA.

To examine the effect of the EP4 agonist, PBMCs from BLV-uninfected cattle were incubated with 1  $\mu$ g/ml Rivenprost, an EP4 agonist (Cayman Chemical). The expression of IFN- $\gamma$  after 24 h of incubation with no additional stimulation was determined by qPCR as described above, and IFN- $\gamma$  concentrations in culture supernatants after 24 h of incubation with 1  $\mu$ g/ml anti-bovine CD3 mAb (MM1A) and 1  $\mu$ g/ml anti-bovine CD28 mAb (CC220) were measured by ELISA as described above. Similarly, IFN- $\gamma$  production in bovine lymphocyte subsets was measured by flow

(D and E) PBMCs from BLV-uninfected cattle ( $n = 12$ ) were incubated with the EP4 agonist in the presence of anti-CD3 mAb, anti-CD28 mAb, and recombinant bovine IL-2. After incubation, IFN- $\gamma$  expression levels in CD4<sup>+</sup> (D) and CD8<sup>+</sup> (E) cells were measured by flow cytometry. (A–E) Statistical significance was determined by the Steel–Dwass test (A) or the Wilcoxon signed-rank test (B–E).

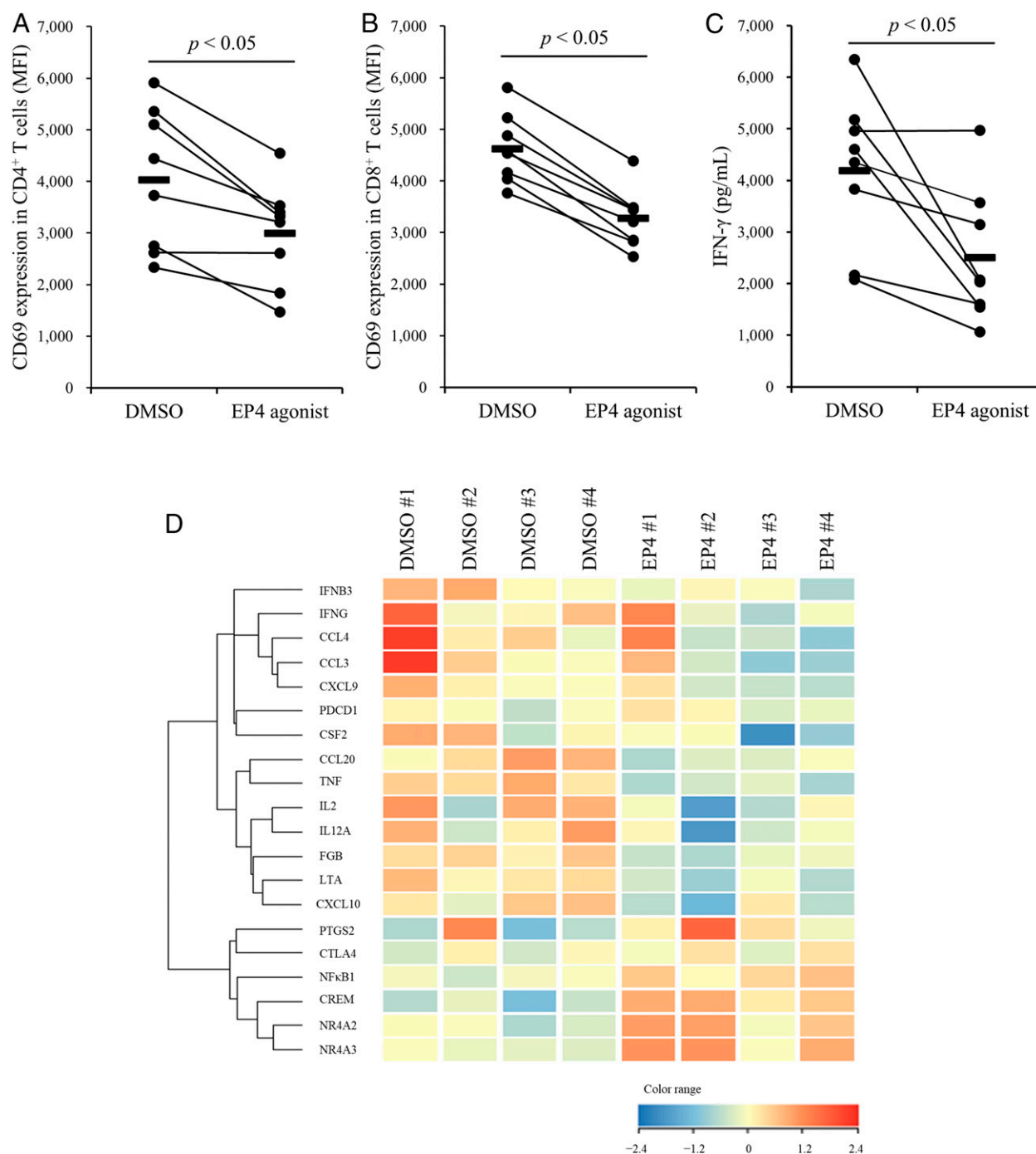


**FIGURE 3. Functional analysis of EP4 signaling in CD3<sup>+</sup> cells.**

(A–C) CD3<sup>+</sup> cells isolated from PBMCs of BLV-uninfected cattle ( $n = 8$ ) were cultured with the EP4 agonist in the presence of anti-CD3 mAb and anti-CD28 mAb. After incubation, CD69 expression levels in CD4<sup>+</sup> (A) and CD8<sup>+</sup> (B) cells and IFN- $\gamma$  concentrations in culture supernatants (C) were measured by flow cytometry and ELISA, respectively. (D) The heat-map for the changes in gene expression levels in CD4<sup>+</sup> cells by the EP4 agonist. (A–C) Statistical significance was determined by the Wilcoxon signed-rank test. MFI, Mean fluorescence intensity.

cytometry by stimulating the cells with 2  $\mu$ g/ml anti-bovine CD3 mAb (MM1A), 2  $\mu$ g/ml anti-bovine CD28 mAb (CC220), and 10 ng/ml recombinant bovine IL-2 (Kingfisher Biotech). Following 19 h of incubation, the cells were incubated with 10  $\mu$ g/ml brefeldin

A (Sigma-Aldrich) for additional 5 h, and analyzed as describe above. To examine the effect of anti-PD-L1 Ab and TNF- $\alpha$  on PGE<sub>2</sub> production, PBMCs from BLV-uninfected cattle were incubated with 10  $\mu$ g/ml anti-bovine PD-L1 Ab (Boch4G12) or 10 ng/ml

TABLE II. The change of gene expression in microarray analysis

| Gene Symbol | Gene Name                                     | Fold Change | p Value  |
|-------------|---|-------------|----------|
| IL2         | IL-2  | -2.1255753  | 0.008147 |
| CCL3        | Chemokine (CC motif) ligand 3                 | -2.0820506  | 0.004651 |
| TNF         | TNF   | -2.0492654  | 0.001460 |
| CSF2        | CSF-2   | -2.0447707  | 0.005276 |
| IL12A       | IL-12A  | -1.9293255  | 0.012709 |
| CXCL10      | CXC motif chemokine ligand 10                 | -1.8574089  | 0.019228 |
| CCL20       | CC motif chemokine ligand 20                  | -1.8484110  | 0.010516 |
| LTA         | Lymphotoxin- $\alpha$                         | -1.8189231  | 0.019710 |
| CCL4        | Chemokine (CC motif) ligand 4                 | -1.7715497  | 0.000768 |
| FGB         | Fibrinogen $\beta$ -chain                     | -1.7014802  | 0.026826 |
| IFNB3       | IFN- $\beta$ 3                                | -1.5604529  | 0.043236 |
| CXCL9       | CXC motif chemokine ligand 9                  | -1.4785548  | 0.000302 |
| IFNG        | IFN- $\gamma$                                 | -1.4232383  | 0.054541 |
| CREM        | cAMP-responsive element modulator             | 2.4109561   | 0.001597 |
| NR4A3       | Nuclear receptor subfamily 4 group A member 3 | 1.9490188   | 0.029402 |
| NR4A2       | Nuclear receptor subfamily 4 group A member 2 | 1.8775752   | 0.001489 |
| PTGS2       | PG-endoperoxide synthase 2                    | 1.7771128   | 0.042600 |
| NFKB1       | NF- $\kappa$ B subunit 1                      | 1.5010872   | 0.001316 |
| CTLA4       | CTL-associated protein 4                      | 1.1734980   | 0.011518 |
| PDCD1       | Programmed cell death 1                       | 1.0657109   | 0.355153 |

bovine rTNF- $\alpha$  (Kingfisher Biotech) for 72 or 24 h, respectively. Bovine IgG (Sigma-Aldrich) was used as a negative control for the anti-PD-L1 Ab Boch4G12, and PBS was used as a vehicle control for bovine rTNF- $\alpha$ . After incubation, the culture supernatants were collected to measure PGE<sub>2</sub> concentrations by ELISA, and the cells were collected for the quantification of COX2 expression by qPCR. Additionally, to investigate whether treatment with anti-PD-L1 Ab induces TNF- $\alpha$  production, PBMCs from BLV-uninfected cattle were incubated with 10  $\mu$ g/ml anti-bovine PD-L1 Ab (Boch4G12) in the presence of 2  $\mu$ g/ml anti-bovine CD3 mAb (MM1A), 2  $\mu$ g/ml anti-bovine CD28 mAb (CC220), and 10 ng/ml recombinant bovine IL-2. Following 19 h of incubation, the cultures were incubated with 10  $\mu$ g/ml brefeldin A for 5 h, after which the cultured PBMCs were harvested, and TNF- $\alpha$  expression levels were measured by flow cytometry. Furthermore, to examine whether the blockade of TNF- $\alpha$  reduces PGE<sub>2</sub> production in the presence of anti-PD-L1 Ab, PBMCs from BLV-uninfected cattle were incubated with 172 nM bovine TNF receptor type II (TNFRII)-Ig, a decoy receptor for bovine TNF- $\alpha$  (35), in the presence of 10  $\mu$ g/ml anti-bovine PD-L1 Ab (Boch4G12). Control Ig, which comprised the signal peptide of bovine TNFRII and the Fc domain of bovine IgG<sub>1</sub> (35), was used as a negative control for TNFRII-Ig. Cultures were stimulated by adding 1  $\mu$ g/ml anti-bovine CD3 mAb (MM1A) and 1  $\mu$ g/ml anti-bovine CD28 mAb (CC220) to each well. After 72 h, the culture supernatants were collected to measure PGE<sub>2</sub> concentrations by ELISA.

To examine the effect of the dual blockade of PD-L1 and EPs in cattle, PBMCs from BLV-uninfected or BLV-infected cattle were cultured with 10  $\mu$ g/ml anti-bovine PD-L1 Ab (Boch4G12) and 1  $\mu$ g/ml each EP antagonist. PBMCs from BLV-uninfected cattle were cultured in the presence of 1  $\mu$ g/ml anti-bovine CD3 mAb (MM1A) and 1  $\mu$ g/ml anti-bovine CD28 mAb (CC220) for 72 h, whereas PBMCs from BLV-infected cattle were cultured in the

presence of a BLV Ag, fetal lamb kidney (FLK)-BLV (2% heat-inactivated culture supernatant of FLK-BLV cells), for 144 h. After incubation, the culture supernatants were collected, and IFN- $\gamma$  concentrations were determined by ELISA.

#### CD3<sup>+</sup> cell culture

Isolated CD3<sup>+</sup> cells were cultured with 1  $\mu$ g/ml the EP4 agonist in the presence of 1  $\mu$ g/ml anti-bovine CD3 mAb (MM1A) and 1  $\mu$ g/ml anti-bovine CD28 mAb (CC220) for 72 h. After incubation, CD69 expression levels and IFN- $\gamma$  concentrations in culture supernatants were measured by flow cytometry and ELISA, respectively.

#### Microarray

Isolated CD4<sup>+</sup> cells were cultured with 0.5  $\mu$ g/ml anti-bovine CD3 mAb (MM1A) and 0.5  $\mu$ g/ml anti-bovine CD28 mAb (CC220). Following 18 h of incubation, the cultures were incubated with 1  $\mu$ g/ml the EP4 agonist or DMSO for 4 h. Microarray analysis was performed using Agilent *Bos taurus* (Bovine) Oligo Microarray v2 (Design ID: 023647; Agilent Technologies, Santa Clara, CA). After cell collection, total RNA was extracted using RNeasy Mini Kit (Qiagen, Hilden, Germany) according to the manufacturer's instructions. Synthesis and labeling of cRNA were performed using Low Input Quick Amp Labeling Kit (Agilent Technologies) according to the manufacturer's instructions. The Cy3-labeled cRNA was purified using RNeasy Mini Kit (Qiagen), and hybridization was performed using Gene Expression Hybridization Kit (Agilent Technologies), according to the manufacturers' instructions. Next, scanning of the hybridized microarray and data analysis were performed using Agilent DNA Microarray Scanner (Agilent Technologies), Feature Extraction software (Agilent Technologies), and GeneSpring (Agilent Technologies), according to the manufacturers' instructions. The microarray data were deposited in ArrayExpress (E-MTAB-9576,

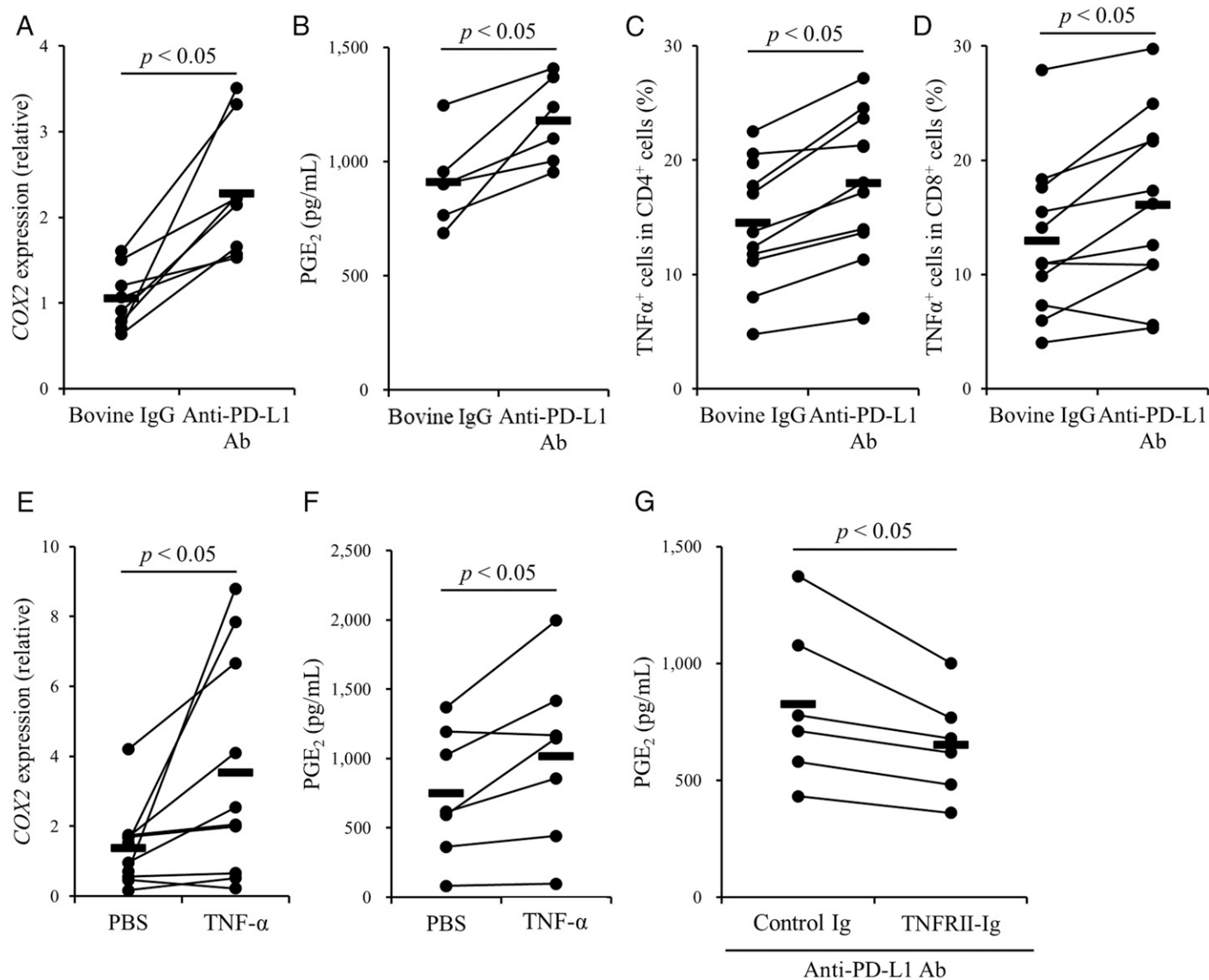


**FIGURE 4. TNF- $\alpha$  induced by PD-L1 blockade upregulates PGE<sub>2</sub> production.**

(A and B) PBMCs from BLV-uninfected cattle were cultured with anti-PD-L1 Ab (Boch4G12), and COX2 expression levels (A,  $n = 8$ ) and PGE<sub>2</sub> concentrations in culture supernatants (B,  $n = 6$ ) were measured by qPCR and ELISA, respectively. Bovine IgG was used as a negative control of anti-PD-L1 Ab (Boch4G12). (C and D) PBMCs from BLV-uninfected cattle ( $n = 11$ ) were incubated with anti-PD-L1 Ab (Boch4G12) in the presence of anti-CD3 mAb, anti-CD28 mAb, and recombinant bovine IL-2. After incubation, TNF- $\alpha$  expression levels in CD4<sup>+</sup> (C) and CD8<sup>+</sup> (D) cells were measured by flow cytometry. (E and F) PBMCs from BLV-uninfected cattle were cultured with recombinant bovine TNF- $\alpha$ , and COX2 expression levels (E,  $n = 10$ ) and PGE<sub>2</sub> concentrations in culture supernatants (F,  $n = 7$ ) were measured by qPCR and ELISA, respectively. PBS was used as a vehicle control. (G) PBMCs from BLV-uninfected cattle ( $n = 6$ ) were cultured with TNFRII-Ig in the presence of anti-PD-L1 Ab (Boch4G12). Cultures were stimulated by adding anti-CD3 mAb and anti-CD28 mAb. Control Ig was used as a negative control for TNFRII-Ig. PGE<sub>2</sub> concentrations in culture supernatants were determined by ELISA. (A–G) Statistical significance was determined by the Wilcoxon signed-rank test.

<https://www.ebi.ac.uk/arrayexpress/>). The microarray procedures from RNA extraction to data analysis were conducted at Hokkaido System Science (Sapporo, Japan).

#### Splenocyte culture

To examine the effects of anti-PD-L1 Ab treatment on PGE<sub>2</sub> production in mice, splenocytes were cultured with 10  $\mu$ g/ml

anti-mouse PD-L1 Ab (10F.9G2; BioXCell, West Lebanon, NH) or 10  $\mu$ g/ml rat IgG<sub>2b</sub> isotype control (LTF-2; BioXCell). PGE<sub>2</sub> concentrations in supernatants of culture incubated with or without 10  $\mu$ g/ml Con A (Sigma-Aldrich) for 72 h were measured by ELISA as described above. To examine the effect of the dual blockade of PD-L1 and EP4 in mice, splenocytes were cultured with 10  $\mu$ g/ml anti-mouse PD-L1 Ab (10F.9G2) and 1  $\mu$ g/ml each

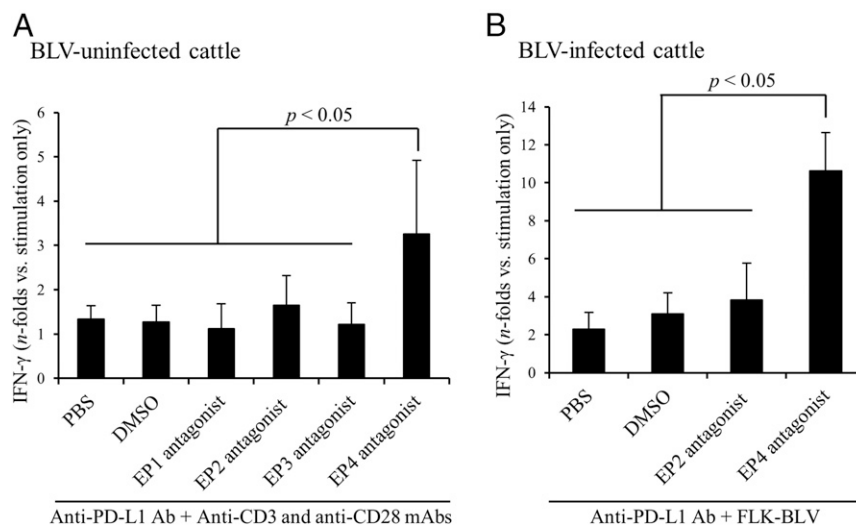


**FIGURE 5. Functional analysis of the dual blockade of PD-L1 and EP4 in cattle.**

(**A** and **B**) PBMCs from BLV-uninfected ( $n = 8$ ) and BLV-infected ( $n = 7$ ) cattle were cultured with anti-PD-L1 Ab (Boch4G12) and indicated EP antagonists. PBMCs from BLV-uninfected cattle were stimulated by anti-CD3 mAb and anti-CD28 mAb. PBMCs from BLV-infected cattle were stimulated by FLK-BLV, a BLV Ag. After incubation, IFN- $\gamma$  concentrations in culture supernatants were measured by ELISA. Statistical significance was determined by the Steel–Dwass test.

EP antagonist. Cultures were stimulated by adding 1  $\mu\text{g}/\text{ml}$  anti-mouse CD3e mAb (145-2C11; Thermo Fisher Scientific) to each well. After 72 h, the culture supernatants were collected, and IL-2 concentrations were measured by ELISA.

#### Tumor grafting and tumor growth measurement

Six-week-old male C57BL/6 mice (Japan SLC, Hamamatsu, Japan) were s.c. inoculated with EG7 ( $5 \times 10^6$  cells per mouse). The day of EG7 injection was defined as day 0. For anti-PD-L1 Ab treatment, mice were i.p. injected with anti-mouse PD-L1 mAb (10F.9G2) (10 mg/kg, once a day) on days 7, 10, and 14. For EP4 antagonist treatment, mice were orally administered with ONO-AE3-208 (10 mg/kg/d) added to drinking water from day 7 to day 23. Tumor size was monitored at least every other day, starting on day 5, using a caliper until the length or width exceeded 20 mm. Tumor volume was calculated according to the following formula: tumor volume ( $\text{mm}^3$ ) = (length  $\times$  width<sup>2</sup>)/2. The animal experiments were performed with the approval of the Institutional Animal Care and Use Committee of the Graduate School of Veterinary Medicine at Hokkaido University (approval number: 16-0131). The animals were handled in accordance with the Guide for the Care and Use of Laboratory Animals, Graduate School of Veterinary Medicine, Hokkaido University (approved by the Association for Assessment and Accreditation of Laboratory Animal Care International).

#### Statistics

In Fig. 1, differences were assessed using the Mann–Whitney  $U$  test. In Figs. 2–5 and 6A–C, differences were assessed using the Wilcoxon signed-rank test for two-group comparisons and the Steel–Dwass test for multiple-group comparisons. In Fig. 6E and

6F, differences were assessed using the Tukey test and the log-rank test, respectively. In microarray analysis (Table II), differences were assessed using the paired  $t$  test. A  $p$  value  $< 0.05$  was considered to indicate statistical significance.

## RESULTS

#### Serum PGE<sub>2</sub> concentration is increased with anti-PD-L1 immunotherapy

We first analyzed the serum samples from BLV-infected cattle that were administered the anti-PD-L1 blocking Ab (Table I) and found that the serum PGE<sub>2</sub> concentrations were increased after the anti-PD-L1 Ab treatment (Fig. 1). Therefore, we specifically examined the role of PGE<sub>2</sub> in the blockade of PD-1/PD-L1 interaction in the current study.

#### T cell activation is suppressed via PGE<sub>2</sub>/EP4 pathway

We have previously shown that PGE<sub>2</sub> suppresses Th1 responses, such as Th1 cytokine production and T cell proliferation, in cattle (30). In the current study, we further aimed to identify specific PGE<sub>2</sub> receptors involved in PGE<sub>2</sub>-mediated immune dysfunction using EP antagonists and agonists. Bovine PBMCs were preincubated with individual EP antagonists, followed by culturing the cells with PGE<sub>2</sub> in the presence of anti-CD3 and anti-CD28 mAbs. Pretreatment with the EP4 antagonist inhibited the suppressive effect of PGE<sub>2</sub>, whereas IFN- $\gamma$  production was suppressed by PGE<sub>2</sub> in PBMCs pretreated with the antagonists of other EPs (EP1–EP3) (Fig. 2A). Additionally, treatment with the EP4 agonist significantly inhibited IFN- $\gamma$  mRNA and its protein expression in PBMCs (Fig. 2B, 2C). Flow cytometric analysis revealed that the

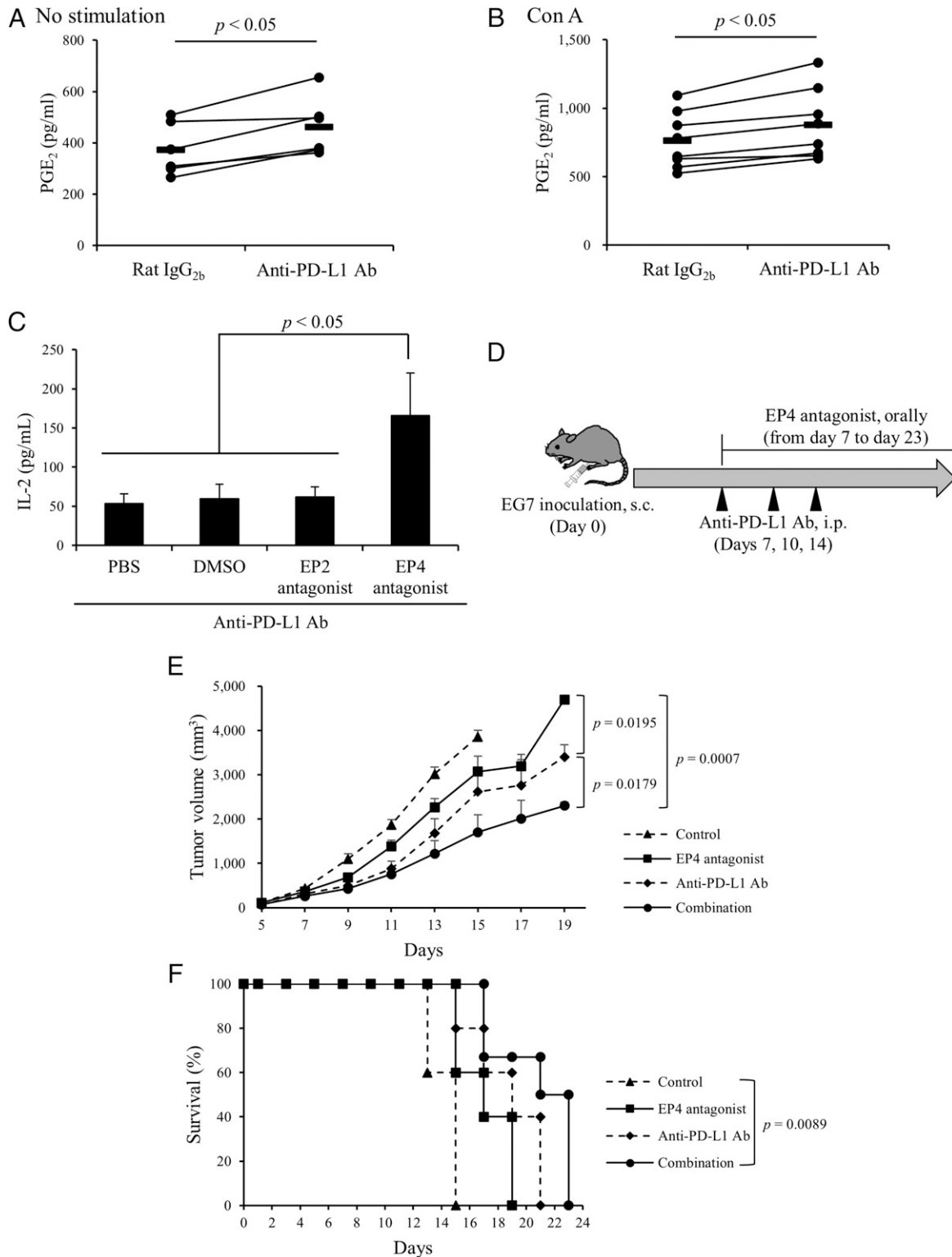


**FIGURE 6. Functional analysis of the dual blockade of PD-L1 and EP4 in mice.**

(A and B) Murine splenocytes (A,  $n = 6$ ; B,  $n = 8$ ) were cultured with anti-PD-L1 Ab (10F.9G2). Cultures were stimulated with or without Con A, and PGE<sub>2</sub> concentrations in culture supernatants were measured by ELISA. Statistical significance was determined by the Wilcoxon signed-rank test. (C) Murine splenocytes ( $n = 6$ ) were cultured with anti-PD-L1 Ab (10F.9G2) and indicated EP antagonists in the presence of anti-mouse CD3e mAb. IL-2 concentrations in culture supernatants were determined by ELISA. Statistical significance was determined by the Steel-Dwass test. (D-F) Evaluation of the antitumor effects of dual blockade in the EG7 mouse model. (D) Experimental design. (E) Tumor growth in each group. **(Continued)**

EP4 agonist decreased the percentage of IFN- $\gamma$ <sup>+</sup> cells in both the CD4<sup>+</sup> and CD8<sup>+</sup> cell populations (Fig. 2D, 2E, Supplemental Fig. 1A, 1B). Furthermore, to examine whether PGE<sub>2</sub> directly suppresses the activity of bovine T cells, isolated CD3<sup>+</sup> T cells were cultured with the EP4 agonist, and the expression levels of CD69, an activation marker, in these cells and IFN- $\gamma$  production in culture supernatants were assayed by flow cytometry and ELISA, respectively. Treatment with the EP4 agonist significantly reduced the CD69 expression levels in CD4<sup>+</sup> and CD8<sup>+</sup> cells and IFN- $\gamma$  production (Fig. 3A–C, Supplemental Fig. 1C, 1D). Microarray analysis revealed that the EP4 agonist treatment downregulated the expression of Th1-related cytokine genes, such as *IL-2*, *IFN- $\gamma$* , *TNF- $\alpha$* , and *IL-12*, in CD4<sup>+</sup> cells (Fig. 3D, Table II). Taken together, these data suggest that PGE<sub>2</sub> induced by PD-L1 blockade directly inhibits T cell activation via the EP4 signaling.

#### ***PD-L1 blockade-mediated induction of TNF- $\alpha$ upregulates PGE<sub>2</sub> production***

As shown in Fig. 1, the serum PGE<sub>2</sub> concentrations were increased after anti-PD-L1 Ab treatment. To examine whether treatment with the anti-PD-L1 Ab induces PGE<sub>2</sub> production in vitro, bovine PBMCs were cultured with anti-PD-L1 Ab (Boch4G12), which significantly induced the *COX2* expression and PGE<sub>2</sub> production in vitro (Fig. 4A, 4B). Blockade of the PD-1/PD-L1 pathway using specific Abs reactivates exhausted T cells, leading to the enhancement of Th1 cytokine production from T cells (5, 6). In the current study, flow cytometric analysis revealed that anti-PD-L1 Ab (Boch4G12) significantly increased the TNF- $\alpha$  expression levels in both CD4<sup>+</sup> and CD8<sup>+</sup> cells (Fig. 4C, 4D, Supplemental Fig. 1A, 1C). Previous reports have clearly demonstrated that TNF- $\alpha$  induces NF- $\kappa$ B activation, which is essential for COX-2 upregulation (36–38). Therefore, we examined whether anti-PD-L1 Ab-induced TNF- $\alpha$  is involved in the observed PGE<sub>2</sub> upregulation. Treatment with bovine rTNF- $\alpha$  significantly induced both the *COX2* expression and PGE<sub>2</sub> production in bovine PBMCs (Fig. 4E, 4F). Interestingly, the blockade of TNF- $\alpha$  using the decoy receptor TNFRII-Ig (35) reduced PGE<sub>2</sub> production in the presence of anti-PD-L1 Ab (Fig. 4G). Collectively, these results suggest that TNF- $\alpha$  induced by PD-L1 blockade upregulates PGE<sub>2</sub> production, contributing to the impaired efficacy of anti-PD-L1 Ab treatment via the PGE<sub>2</sub>/EP4 signaling.

#### ***Th1 cytokine production is enhanced by the dual blockade of PD-L1 and EP4***

To examine whether the inhibition of EP4 enhances the efficacy of anti-PD-L1 Ab in vitro, bovine PBMCs were cultured with individual EP antagonists in the presence of anti-PD-L1 Ab (Boch4G12). As shown in Fig. 5A, the dual blockade of PD-L1 and EP4 increased IFN- $\gamma$  production compared with other treatment

groups. Additionally, the dual blockade of PD-L1 and EP4 significantly enhanced the BLV-specific IFN- $\gamma$  production from PBMCs of BLV-infected cattle (Fig. 5B). Taken together, these results suggest that combination with an EP4 antagonist might be a novel strategy to enhance the efficacy of anti-PD-L1 Ab treatment in cattle.

#### ***Antitumor effects are enhanced by the dual blockade of PD-L1 and EP4***

Our studies in bovine immune cells revealed the novel mechanism of anti-PD-L1 Ab resistance and the potential of enhancing Th1 cytokine production by the dual blockade of PD-L1 and EP4. We then used murine splenocytes to examine whether the dual blockade enhances Th1 immune responses in other animal models. As shown in Fig. 6A and 6B, anti-PD-L1 Ab induced PGE<sub>2</sub> production from murine splenocytes stimulated with or without Con A (Fig. 6A, 6B). Additionally, treatment with the EP4 antagonist increased IL-2 production from murine splenocytes in the presence of anti-PD-L1 Ab (10F.9G2) (Fig. 6C), suggesting that the dual blockade enhanced Th1 responses not only in cattle but also in mice. Finally, based on these results, we used a mouse lymphoma model to evaluate the potential antitumor effects of the dual blockade as a potent immunotherapy in cancers resistant to anti-PD-1/PD-L1 Ab alone. C57BL/6 mice were inoculated with a lymphoma cell line, EG7, and the EG7-bearing mice were administered anti-PD-L1 Ab (10F.9G2) i.p. and the EP4 antagonist orally (Fig. 6D). Compared with the animals treated with the EP4 antagonist or the anti-PD-L1 Ab alone, the growth of EG7 cells was inhibited in those administered the combination treatment (Fig. 6E). Additionally, the survival of the combination treatment group was significantly prolonged compared with that of the untreated group (Fig. 6F). Taken together, these data suggest that the dual blockade of PD-L1 and EP4 is a promising strategy as a novel immunotherapy.

## **DISCUSSION**

Numerous studies have recently elucidated the mechanisms of resistance to cancer immunotherapy (39–41). For instance, Koyama et al. (39) demonstrated that therapeutic PD-1 blockade upregulated the expression of alternative immune checkpoint molecules, which caused resistance to the PD-1/PD-L1 blockade. Treatments including anti-PD-1/PD-L1 Abs in combination with other medicines to overcome resistance are garnering increasing attention. Previous studies have shown that combination treatment with anti-PD-1/PD-L1 Abs with COX inhibitors enhances the therapeutic efficacy in murine and bovine models (12, 32). However, the mechanisms underlying the observed therapeutic

Data are presented as means, and the error bars indicate SEs. Statistical significance was determined by the Tukey test. (F) The Kaplan–Meier Curve for survival in all groups. Statistical significance was determined by the log-rank test. (D–F) Data are representative of two independent experiments, each performed with five to eight mice per group.

effect of these combination approaches remain unclear. In the current study, we identify a novel mechanism of resistance related to PGE<sub>2</sub> using a bovine model (Supplemental Fig. 2). It was revealed that the anti-PD-L1 Ab treatment induced the production of Th1 cytokines, such as TNF- $\alpha$ , and that TNF- $\alpha$ -induced PGE<sub>2</sub> suppressed the activation of T cells via EP4. This might partially explain a reason that the combined treatment enhances the efficacy of anti-PD-1/PD-L1 Abs. In addition, our study clearly showed the therapeutic potential of combination treatment with anti-PD-L1 Abs and EP4 antagonists in bovine and murine models. To the best of our knowledge, this is the first study to demonstrate the therapeutic efficacy of a dual blockade strategy using an anti-PD-L1 Ab and an EP4 antagonist in an *in vivo* model. Future studies in other murine tumor models are warranted to further investigate the efficacy of the dual blockade.

Among the four PGE<sub>2</sub> receptors EP1-4 (20), EP2 and EP4 are involved in PGE<sub>2</sub>-associated immune dysfunction (21). In the current study, the blockade of EP4, but not EP2, inhibited the suppression of IFN- $\gamma$  production by PGE<sub>2</sub>. EP4 is a high-affinity receptor for PGE<sub>2</sub>, whereas EP2 requires significantly higher PGE<sub>2</sub> concentrations for effective signaling (21). Thus, the observed differences in the results following the blockade of EP2 and EP4 might be due to the difference in the affinity of each receptor. The contribution of EP2 to immunosuppression should carefully be investigated in other preclinical models in which higher PGE<sub>2</sub> levels are expected during disease progression.

Anti-PD-1/PD-L1 Abs reactivate exhausted T cells, leading to the production of Th1 cytokines, such as IFN- $\gamma$  and TNF- $\alpha$  (5, 6). TNF- $\alpha$  not only plays a critical role in cellular immunity against cancer, but also has a direct cytotoxic effect on tumor cells by inducing apoptosis (42, 43). Although known as an antitumor cytokine, TNF- $\alpha$  paradoxically promotes tumor progression in some circumstances (44-46). For example, serum TNF- $\alpha$  concentration is correlated with the progression of several cancer types, such as renal cell carcinoma and prostate cancer (47, 48). Additionally, the blockade of TNF- $\alpha$  using Abs inhibits tumor growth (49). Furthermore, recent studies have shown that the blockade of TNF- $\alpha$  improves the efficacy of PD-1 blockade (50, 51); however, the underlying detailed mechanism has not been fully elucidated. In the current study, we demonstrated that TNF- $\alpha$  was involved in PGE<sub>2</sub> upregulation under anti-PD-L1 Ab treatment, and that the dual blockade of PD-1/PD-L1 and EP4 enhanced the efficacy of immunotherapy. Our strategy might be more effective than the dual blockade of PD-1/PD-L1 and TNF- $\alpha$  because the antitumor effects of TNF- $\alpha$  are not inhibited. Further studies are necessary to compare the efficacy between the two strategies.

PGE<sub>2</sub>/EP4 signaling increases cAMP production (52). One study has previously shown that the PGE<sub>2</sub>/EP4/cAMP upregulates the expression of T cell Ig and mucin domain-3 (TIM-3), an immunoinhibitory molecule, in a human T cell line (53). Additionally, several reports have investigated that TIM-3 expression is induced after the PD-1/PD-L1 blockade, leading to the resistance to PD-1/PD-L1 blockade (39, 50). Therefore, PGE<sub>2</sub> upregulation after the PD-1/PD-L1 blockade might also contribute to resistance via the upregulation of other immunoinhibitory molecules.

PD-L1 blockade-TNF- $\alpha$ -PGE<sub>2</sub>-EP4 axis is a novel mechanism of resistance to anti-PD-1/PD-L1 immunotherapy. A novel combined approach targeting PD-L1 and EP4 as immunotherapy may overcome resistance to the anti-PD-1/PD-L1 Ab therapy. Further studies using different murine tumor models as well as other animal models will herald new avenues for cancer treatment.

## DISCLOSURES

The authors have no financial conflicts of interest.

## ACKNOWLEDGMENTS

We thank Dr. Hideyuki Takahashi, Dr. Yasuyuki Mori, and Dr. Tomio Ibayashi for valuable advice and discussions. We thank Enago ([www.enago.jp](http://www.enago.jp)) for the English language review.

## REFERENCES

- Okazaki, T., and T. Honjo. 2007. PD-1 and PD-1 ligands: from discovery to clinical application. *Int. Immunol.* 19: 813-824.
- Blank, C., T. F. Gajewski, and A. Mackensen. 2005. Interaction of PD-L1 on tumor cells with PD-1 on tumor-specific T cells as a mechanism of immune evasion: implications for tumor immunotherapy. *Cancer Immunol. Immunother.* 54: 307-314.
- Blank, C., and A. Mackensen. 2007. Contribution of the PD-L1/PD-1 pathway to T-cell exhaustion: an update on implications for chronic infections and tumor evasion. *Cancer Immunol. Immunother.* 56: 739-745.
- Iwai, Y., M. Ishida, Y. Tanaka, T. Okazaki, T. Honjo, and N. Minato. 2002. Involvement of PD-L1 on tumor cells in the escape from host immune system and tumor immunotherapy by PD-L1 blockade. *Proc. Natl. Acad. Sci. USA* 99: 12293-12297.
- Keir, M. E., M. J. Butte, G. J. Freeman, and A. H. Sharpe. 2008. PD-1 and its ligands in tolerance and immunity. *Annu. Rev. Immunol.* 26: 677-704.
- Dulos, J., G. J. Carven, S. J. van Boxtel, S. Evers, L. J. Driessen-Engels, W. Hobo, M. A. Gorecka, A. F. de Haan, P. Mulders, C. J. Punt, et al. 2012. PD-1 blockade augments Th1 and Th17 and suppresses Th2 responses in peripheral blood from patients with prostate and advanced melanoma cancer. *J. Immunother.* 35: 169-178.
- Iwai, Y., J. Hamanishi, K. Chamoto, and T. Honjo. 2017. Cancer immunotherapies targeting the PD-1 signaling pathway. *J. Biomed. Sci.* 24: 26.
- Ribas, A., and J. D. Wolchok. 2018. Cancer immunotherapy using checkpoint blockade. *Science* 359: 1350-1355.
- Nishimori, A., S. Konnai, T. Okagawa, N. Maekawa, R. Ikebuchi, S. Goto, Y. Sajiki, Y. Suzuki, J. Kohara, S. Ogasawara, et al. 2017. *In vitro* and *in vivo* antiviral activity of an anti-programmed death-ligand 1 (PD-L1) rat-bovine chimeric antibody against bovine leukemia virus infection. *PLoS One* 12: e0174916.
- Okagawa, T., S. Konnai, A. Nishimori, N. Maekawa, R. Ikebuchi, S. Goto, C. Nakajima, J. Kohara, S. Ogasawara, Y. Kato, et al. 2017. Anti-bovine programmed death-1 rat-bovine chimeric antibody for immunotherapy of bovine leukemia virus infection in cattle. *Front. Immunol.* 8: 650.
- Maekawa, N., S. Konnai, S. Takagi, Y. Kagawa, T. Okagawa, A. Nishimori, R. Ikebuchi, Y. Izumi, T. Deguchi, C. Nakajima, et al. 2017. A canine chimeric monoclonal antibody targeting PD-L1 and its clinical efficacy in canine oral malignant melanoma or undifferentiated sarcoma. *Sci. Rep.* 7: 8951.

12. Sajiki, Y., S. Konnai, T. Okagawa, A. Nishimori, N. Maekawa, S. Goto, K. Watari, E. Minato, A. Kobayashi, J. Kohara, et al. 2019. Prostaglandin E<sub>2</sub>-induced immune exhaustion and enhancement of antiviral effects by anti-PD-L1 antibody combined with COX-2 inhibitor in bovine leukemia virus infection. *J. Immunol.* 203: 1313–1324.
13. Goto, S., S. Konnai, Y. Hirano, J. Kohara, T. Okagawa, N. Maekawa, Y. Sajiki, K. Watari, E. Minato, A. Kobayashi, et al. 2020. Clinical efficacy of the combined treatment of anti-PD-L1 rat-bovine chimeric antibody with a COX-2 inhibitor in calves infected with *Mycoplasma bovis*. *Jpn. J. Vet. Res.* 68: 77–90.
14. Sagata, N., T. Yasunaga, J. Tsuzuku-Kawamura, K. Ohishi, Y. Ogawa, and Y. Ikawa. 1985. Complete nucleotide sequence of the genome of bovine leukemia virus: its evolutionary relationship to other retroviruses. *Proc. Natl. Acad. Sci. USA* 82: 677–681.
15. Schwartz, I., and D. Lévy. 1994. Pathobiology of bovine leukemia virus. *Vet. Res.* 25: 521–536.
16. Gong, J., A. Chehrizi-Raffle, S. Reddi, and R. Salgia. 2018. Development of PD-1 and PD-L1 inhibitors as a form of cancer immunotherapy: a comprehensive review of registration trials and future considerations. *J. Immunother. Cancer* 6: 8.
17. Phipps, R. P., S. H. Stein, and R. L. Roper. 1991. A new view of prostaglandin E regulation of the immune response. *Immunol. Today* 12: 349–352.
18. Subbaramaiah, K., N. Telang, J. T. Ramonetti, R. Araki, B. DeVito, B. B. Weksler, and A. J. Dannenberg. 1996. Transcription of cyclooxygenase-2 is enhanced in transformed mammary epithelial cells. *Cancer Res.* 56: 4424–4429.
19. Morita, I. 2002. Distinct functions of COX-1 and COX-2. *Prostaglandins Other Lipid Mediat.* 68–69: 165–175.
20. Sugimoto, Y., and S. Narumiya. 2007. Prostaglandin E receptors. *J. Biol. Chem.* 282: 11613–11617.
21. Kalinski, P. 2012. Regulation of immune responses by prostaglandin E<sub>2</sub>. *J. Immunol.* 188: 21–28.
22. Kobayashi, K., K. Omori, and T. Murata. 2018. Role of prostaglandins in tumor microenvironment. *Cancer Metastasis Rev.* 37: 347–354.
23. Tomozawa, S., N. H. Tsuno, E. Sunami, K. Hatano, J. Kitayama, T. Osada, S. Saito, T. Tsuruo, Y. Shibata, and H. Nagawa. 2000. Cyclooxygenase-2 overexpression correlates with tumour recurrence, especially haematogenous metastasis, of colorectal cancer. *Br. J. Cancer* 83: 324–328.
24. Denkert, C., K. J. Winzer, B. M. Müller, W. Weichert, S. Pest, M. Köbel, G. Kristiansen, A. Reles, A. Siegert, H. Guski, and S. Hauptmann. 2003. Elevated expression of cyclooxygenase-2 is a negative prognostic factor for disease free survival and overall survival in patients with breast carcinoma. *Cancer* 97: 2978–2987.
25. Rigas, B., I. S. Goldman, and L. Levine. 1993. Altered eicosanoid levels in human colon cancer. *J. Lab. Clin. Med.* 122: 518–523.
26. Wang, D., H. Wang, Q. Shi, S. Katkuri, W. Walhi, B. Desvergne, S. K. Das, S. K. Dey, and R. N. DuBois. 2004. Prostaglandin E<sub>2</sub> promotes colorectal adenoma growth via transactivation of the nuclear peroxisome proliferator-activated receptor delta. *Cancer Cell* 6: 285–295.
27. Wang, D., and R. N. DuBois. 2010. Eicosanoids and cancer. *Nat. Rev. Cancer* 10: 181–193.
28. Li, H., M. L. Edin, A. Gruzdev, J. Cheng, J. A. Bradbury, J. P. Graves, L. M. DeGraff, and D. C. Zeldin. 2013. Regulation of T helper cell subsets by cyclooxygenases and their metabolites. *Prostaglandins Other Lipid Mediat.* 104–105: 74–83.
29. Prima, V., L. N. Kaliberova, S. Kaliberov, D. T. Curiel, and S. Kusmartsev. 2017. COX2/mPGES1/PGE<sub>2</sub> pathway regulates PD-L1 expression in tumor-associated macrophages and myeloid-derived suppressor cells. *Proc. Natl. Acad. Sci. USA* 114: 1117–1122.
30. Sajiki, Y., S. Konnai, T. Okagawa, A. Nishimori, N. Maekawa, S. Goto, R. Ikebuchi, R. Nagata, S. Kawaji, Y. Kagawa, et al. 2018. Prostaglandin E<sub>2</sub> induction suppresses the Th1 immune responses in cattle with Johne's disease. *Infect. Immun.* 86: e00910–e00917.
31. Goto, S., S. Konnai, Y. Hirano, J. Kohara, T. Okagawa, N. Maekawa, Y. Sajiki, K. Watari, E. Minato, A. Kobayashi, et al. 2020. Upregulation of PD-L1 expression by prostaglandin E<sub>2</sub> and the enhancement of IFN- $\gamma$  by anti-PD-L1 antibody combined with a COX-2 inhibitor in *Mycoplasma bovis* infection. *Front. Vet. Sci.* 7: 12.
32. Zelenay, S., A. G. van der Veen, J. P. Böttcher, K. J. Snelgrove, N. Rogers, S. E. Acton, P. Chakravarty, M. R. Girotti, R. Marais, S. A. Quezada, et al. 2015. Cyclooxygenase-dependent tumor growth through evasion of immunity. *Cell* 162: 1257–1270.
33. Sajiki, Y., S. Konnai, A. Nishimori, T. Okagawa, N. Maekawa, S. Goto, M. Nagano, J. Kohara, N. Kitano, T. Takahashi, et al. 2017. Intrauterine infection with bovine leukemia virus in pregnant dam with high viral load. *J. Vet. Med. Sci.* 79: 2036–2039.
34. Moore, M. W., F. R. Carbone, and M. J. Bevan. 1988. Introduction of soluble protein into the class I pathway of antigen processing and presentation. *Cell* 54: 777–785.
35. Fujisawa, S., S. Konnai, T. Okagawa, N. Maekawa, A. Tanaka, Y. Suzuki, S. Murata, and K. Ohashi. 2019. Effects of bovine tumor necrosis factor alpha decoy receptors on cell death and inflammatory cytokine kinetics: potential for bovine inflammation therapy. *BMC Vet. Res.* 15: 68.
36. Jobin, C., O. Morteau, D. S. Han, and R. Balfour Sartor. 1998. Specific NF-kappaB blockade selectively inhibits tumour necrosis factor-alpha-induced COX-2 but not constitutive COX-1 gene expression in HT-29 cells. *Immunology* 95: 537–543.
37. Ghosh, S., and M. Karin. 2002. Missing pieces in the NF-kappaB puzzle. *Cell* 109(Suppl): S81–S96.
38. Bouwmeester, T., A. Bauch, H. Ruffner, P. O. Angrand, G. Bergamini, K. Croughton, C. Cruciat, D. Eberhard, J. Gagneur, S. Ghidelli, et al. 2004. A physical and functional map of the human TNF-alpha/NF-kappa B signal transduction pathway. [Published erratum appears in 2004 *Nat. Cell Biol.* 6: 465.] *Nat. Cell Biol.* 6: 97–105.
39. Koyama, S., E. A. Akbay, Y. Y. Li, G. S. Herter-Sprie, K. A. Buczkowski, W. G. Richards, L. Gandhi, A. J. Redig, S. J. Rodig, H. Asahina, et al. 2016. Adaptive resistance to therapeutic PD-1 blockade is associated with upregulation of alternative immune checkpoints. *Nat. Commun.* 7: 10501.
40. Sharma, P., S. Hu-Lieskovan, J. A. Wargo, and A. Ribas. 2017. Primary, adaptive, and acquired resistance to cancer immunotherapy. *Cell* 168: 707–723.
41. Nowicki, T. S., S. Hu-Lieskovan, and A. Ribas. 2018. Mechanisms of resistance to PD-1 and PD-L1 blockade. *Cancer J.* 24: 47–53.
42. Goodsell, D. S. 2006. The molecular perspective: tumor necrosis factor. *Oncologist* 11: 83–84.
43. Tamada, K., and L. Chen. 2006. Renewed interest in cancer immunotherapy with the tumor necrosis factor superfamily molecules. *Cancer Immunol. Immunother.* 55: 355–362.
44. Moore, R. J., D. M. Owens, G. Stamp, C. Arnott, F. Burke, N. East, H. Holdsworth, L. Turner, B. Rollins, M. Pasparakis, et al. 1999. Mice deficient in tumor necrosis factor-alpha are resistant to skin carcinogenesis. *Nat. Med.* 5: 828–831.
45. Balkwill, F. 2006. TNF- $\alpha$  in promotion and progression of cancer. *Cancer Metastasis Rev.* 25: 409–416.
46. Szlosarek, P., K. A. Charles, and F. R. Balkwill. 2006. Tumour necrosis factor-alpha as a tumour promoter. *Eur. J. Cancer* 42: 745–750.
47. Yoshida, N., S. Ikemoto, K. Narita, K. Sugimura, S. Wada, R. Yasumoto, T. Kishimoto, and T. Nakatani. 2002. Interleukin-6, tumour necrosis factor alpha and interleukin-1beta in patients with renal cell carcinoma. *Br. J. Cancer* 86: 1396–1400.
48. Michalaki, V., K. Syrigos, P. Charles, and J. Waxman. 2004. Serum levels of IL-6 and TNF-alpha correlate with clinicopathological features and patient survival in patients with prostate cancer. [Published erratum appears in 2004 *Br. J. Cancer* 91: 1227.] *Br. J. Cancer* 90: 2312–2316.

49. Scott, K. A., R. J. Moore, C. H. Arnott, N. East, R. G. Thompson, B. J. Scallon, D. J. Shealy, and F. R. Balkwill. 2003. An anti-tumor necrosis factor-alpha antibody inhibits the development of experimental skin tumors. *Mol. Cancer Ther.* 2: 445-451.
50. Bertrand, F., A. Montfort, E. Marcheteau, C. Imbert, J. Gilhodes, T. Filleron, P. Rochaix, N. Andrieu-Abadie, T. Levade, N. Meyer, et al. 2017. TNF $\alpha$  blockade overcomes resistance to anti-PD-1 in experimental melanoma. *Nat. Commun.* 8: 2256.
51. Perez-Ruiz, E., L. Minute, I. Otano, M. Alvarez, M. C. Ochoa, V. Belsue, C. de Andrea, M. E. Rodriguez-Ruiz, J. L. Perez-Gracia, I. Marquez-Rodas, et al. 2019. Prophylactic TNF blockade uncouples efficacy and toxicity in dual CTLA-4 and PD-1 immunotherapy. *Nature* 569: 428-432.
52. Yokoyama, U., K. Iwatsubo, M. Umemura, T. Fujita, and Y. Ishikawa. 2013. The prostanoid EP4 receptor and its signaling pathway. *Pharmacol. Rev.* 65: 1010-1052.
53. Yun, S. J., B. Lee, K. Komori, M. J. Lee, B. G. Lee, K. Kim, and S. Park. 2019. Regulation of TIM-3 expression in a human T cell line by tumor-conditioned media and cyclic AMP-dependent signaling. *Mol. Immunol.* 105: 224-232.